

# Design of graphene-based multi-input multi-output antenna for 6G/IoT applications

Reem Hikmat Abd, Hussein A. Abdulnabi

Department of Electrical Engineering, College of Engineering, Al-Mustansiriyah University, Baghdad, Iraq

## Article Info

### Article history:

Received Nov 30, 2022

Revised Mar 9, 2023

Accepted Mar 12, 2023

### Keywords:

6G communications

Graphene

MIMO antenna

Terahertz

Wireless

## ABSTRACT

In the future, 6G wireless communications will be integrated into various applications. It is expected that it will handle all Internet of Things services as well as satellite communications. Additionally, it is predicted to support machine learning (ML) and artificial intelligence (AI). So this work investigated four orthogonal ports graphene-based multiple-input and multiple-output (MIMO) antenna in the terahertz frequency regime. With wide-band (7.1-13) THz, minimum return loss close to -30 dB and a good isolation value. That was designed over silicon dioxide (SiO<sub>2</sub>) 100×100 substrate with a thickness of 10 μm and a maximum gain reaching 8.3 dB at 11 THz. By adjusting the provided DC voltage, the chemical potential of graphene can be tuned, which in turn allows for the MIMO antenna characteristics to be changed. Envelop correlation coefficient (ECC) and diversity gain (DG) were investigated for the presented design. In addition, these values were determined to assess compatibility and difficulties connected with communication over a short distance. The geometry of the MIMO antenna is adaptable to various applications in the THz band with high-performance requirements, such as sensing, scanning for security threats, biomedical applications, wireless communication systems with high speed built on the 6G standard, and the internet of things (IoT).

This is an open access article under the [CC BY-SA](https://creativecommons.org/licenses/by-sa/4.0/) license.



## Corresponding Author:

Reem Hikmat Abd

Department of Electrical Engineering, College of Engineering, Al-Mustansiriyah University

Baghdad, Iraq

Email: reem.engineer89@gmail.com

## 1. INTRODUCTION

Modern wireless communication system has increased the demand for greater transmission capacity, a high bandwidth, and enhanced usage of the existing frequency range. The most technical development is using numerous antenna elements at both network endpoints. These are known as wireless systems: multiple-input and multiple-output (MIMO) [1]. It provides a higher data rate without requiring additional transmit power or bandwidth [2]. MIMO was first proposed as a valid technology in the early 1990s. A solution capable of overcoming the data rate restriction systems with a single input and one single output (SISO).

The separation between the elements significantly influences the mutual coupling between the antenna elements in a MIMO antenna. As a result of closer separation, the more mutual coupling will cause high correlation coefficients and lower gain and efficiency [3]. Further, MIMO can be employed in various networks to enhance system dependability, data transmission speed and channel performance [4]. Over the past several years, as the need for ultra-high-speed connectivity and higher data rates has grown, a new age of the 6G wireless communication technology has garnered considerable attention. And around 2030 that it will be ready for use [5].

As one of its most important building blocks, the 6G wireless communication infrastructure will require frequency bands operating at terahertz (THz) frequencies. Due to the lack of available sources, measurements, detectors, materials, and equipment that can function inside the terahertz band, The 6G evolution in the terahertz frequency range got the slightest investigation of all electromagnetic spectrum bands [6], [7]. Terahertz wireless communications may be the future wireless technology to overcome the requirements of the increased channel capacity and Tbps data rate [8].

The THz spectrum spans the frequency range from 0.1 to 10 THz and can be found between microwave and infrared spectrums [9]. Recent years have seen an increase in the use of the terahertz frequency spectrum for various purposes, including high data rate transmission in the internet of things (IoT) applications, medicinal applications [10], material characterizations, high-speed [11], and secure data transfer. THz applications, including imaging, spectroscopy, and others, have significantly increased in the last few years [12].

When measured at THz frequencies, the conductivity of the metal is lower than it is when measured at direct current (DC) frequencies; this allows for greater penetration and lowers radiation efficiency produced by metallic antennas when operating at THz frequencies scales [13]. Antennas operating at THz frequencies are often constructed from metals such as gold. Investigation into non-metallic materials use is recommended to reduce losses in smaller antennas.

At this time, graphene is utilized as the material of choice to minimize losses in the THz area [14]. Graphene has a honeycomb lattice structure in two dimensions. It possesses the highest carrier mobility, more significant than 100,000 cm<sup>2</sup>v<sup>-1</sup>s<sup>-1</sup>at room temperature [11]. Its complex surface conductivity is regulated by chemical doping or a change in gate voltage [15].

Graphene's mechanical qualities are very noteworthy. It is very lightweight, durable, and flexible. It was denser than diamond and more than 300 times stronger than steel [16]. It has been the subject of the most in-depth research due to its 2D crystal structure-derived remarkable properties, including its strength, conductivity, and high carrier mobility [3]. It is utilized in multiple applications, such as metamaterials, transparent solar cells, and high-speed transistors [4]. Graphene is used as a radiating patch antenna, a high-impedance surface (HIS) or a parasitic component in the construction of THz [17].

## 2. METHOD

### 2.1. Graphene conductivity

Graphene is a two-dimensional material with one atomic thickness [18]. The graphene surface conductivity can be divided into two parts: the first is referred to as the intra-band dominates in the frequency range of less than five terahertz (THz), and the second is the inter-band dominates at higher frequencies. Both parts of the graphene surface conductivity are affected by the chemical potential, frequency, temperatures and scattering rate shown in (1)-(3) [19]:

$$\sigma = \sigma_{inter} + \sigma_{intra} \tag{1}$$

$$\sigma_{intra}(\omega, T, \mu_c, \gamma) = \frac{e^2 k_B T \tau}{\pi \hbar^2} \left[ \frac{\mu_c}{k_B T} + 2 \ln \left( e^{\frac{-\mu_c}{k_B T}} + 1 \right) \right] \frac{1}{\omega - j2\gamma} \tag{2}$$

$$\sigma_{inter}(\omega, T, \mu_c, \gamma) = \frac{-je^2}{4\pi\hbar} \ln \left( \frac{2|\mu_c| - (\omega - j2\gamma)\hbar}{2|\mu_c| + (\omega - j2\gamma)\hbar} \right) \tag{3}$$

$\mu_c$  is the chemical potential in eV,  $e$  is the Electron charge,  $\omega$  is the Angular frequency in rad/sec,  $T$  is the temperature in Kelvin,  $\gamma$  is the Scattering rate in s<sup>-1</sup>,  $k_B$  is the Boltzmann constant, and  $\hbar$  is Planck's constant.

As shown in (4) makes it possible to calculate the surface impedance of graphene-based on its conductivity [20].

$$Z_{S=1/\sigma(\omega)} = R_S(V_b) + j X_S(V_b) \tag{4}$$

Figure 1 represented graphene's conductivity as a function of rising chemical potential, with solid lines representing the real conductivity and dashed lines representing the imaginary conductivity. The negative real component of graphene's conductivity demonstrates its metal-like behaviour in the mid-infrared spectrum. The conductivity changes toward increasingly negative values as the Fermi level rises.

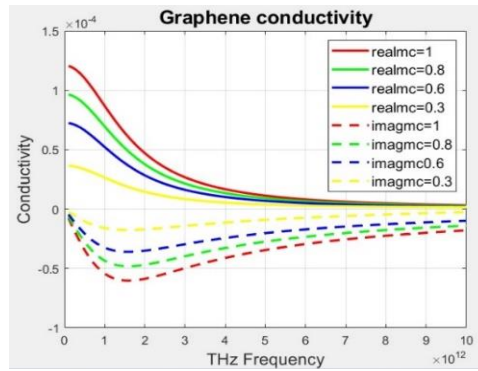


Figure 1. Graphene conductivity plotted as a function of increasing chemical potential

**2.2. The single antenna designed**

Figure 2 illustrates the geometry of the square-patch slotted antenna. Figure 2(a) presents a microstrip with a square patch (28×28 μm<sup>2</sup>) and four slots are etched in the middle of the X and Y axes. These slots are identical in width and length. And also cut, four small slots in each rectangular axes appear. With background enhanced to improve the return loss and the gain, as shown in Figure 2(b).

The antenna made from graphene element thickness of 0.001 nm and a relaxation time of 0.1 ps is printed on the front surface of the silicon dioxide dielectric substrate (SiO<sub>2</sub>) 42×50 μm<sup>2</sup> with ε<sub>r</sub>=3.9 and a height of 10 μm, two layers above the substrate silicon crystalline and alumina with a thickness of 1μm as represented in Figure 2(c). All optimum dimensions of the single antenna are described in Table 1.

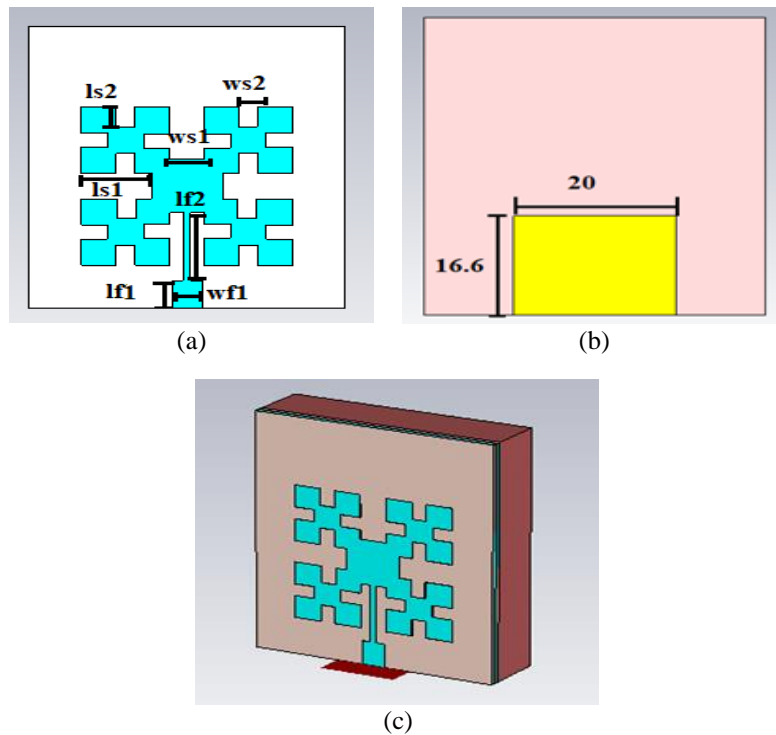


Figure 2. The designed microstrip antenna (a) the front view (b) the back view, and (c) the 3-D view

Table 1. The dimensions of the single antenna design

Parameters	Value in μm	Parameters	Value in μm
ls1	9.3	ws1	4.5
ls2	3	ws2	2.5
lf1	5	wf1	4
lf2	12	wf2	1

The full-wave electromagnetic computer simulation technology (CST 2020) is used for optimizing and designing the proposed antenna. Using the stated mathematical formulas in [21]-[24]. The primary antenna configuration operates at (7.17-12.1) THz, illustrated in Figure 3. Figure 4 represents the simulated radiation patterns of the proposed antenna in the (Y-Z plane) E-plane and (X-Z plane) H-plane. Figure 5 shows the gain of IEEE reaching 9.7 dB at 11 THz, respectively.

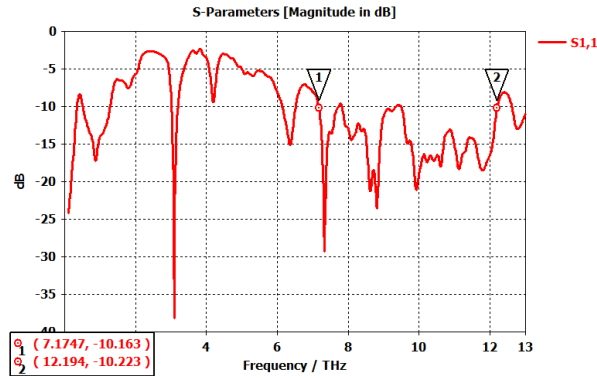


Figure 3. Reflection coefficient  $S_{11}$

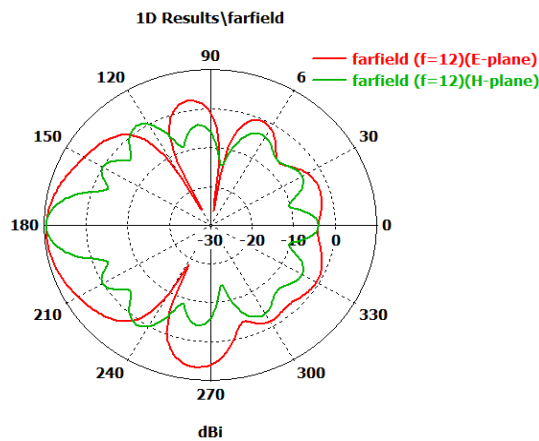


Figure 4. The radiation pattern at F=12 THz

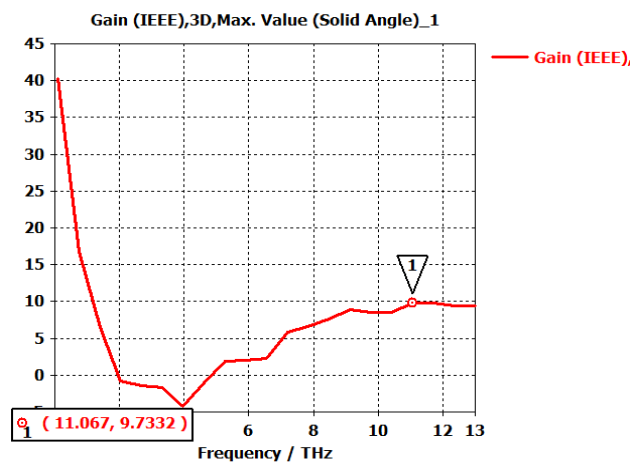


Figure 5. The gain IEEE

### 2.3. The MIMO antenna design

Figure 6 illustrates the suggested design of the MIMO antenna, modified from a single-antenna to a four-port MIMO antenna, arranged orthogonally and placed on the top side of the silicon dioxide (SiO<sub>2</sub>) substrate as represented in Figure 6(a) with an enhanced background as described in Figure 6(b). A ten  $\mu\text{m}$  thickness is illustrated in Figure 6(c). The total dimensions of the MIMO antenna are  $100 \times 100 \mu\text{m}^2$ . The microstrip feed line is linked at the lower borders of each radiator to increase the isolation and reduce the effect of the transmission coefficient by making all of the ports orthogonal and aligned at 90 degrees. The increase in antenna number increases bandwidth and gain; the distance between each antenna is  $30 \mu\text{m}$  according to ( $\lambda/2$ ) to decrease the mutual coupling and enhances the MIMO antenna's performance.

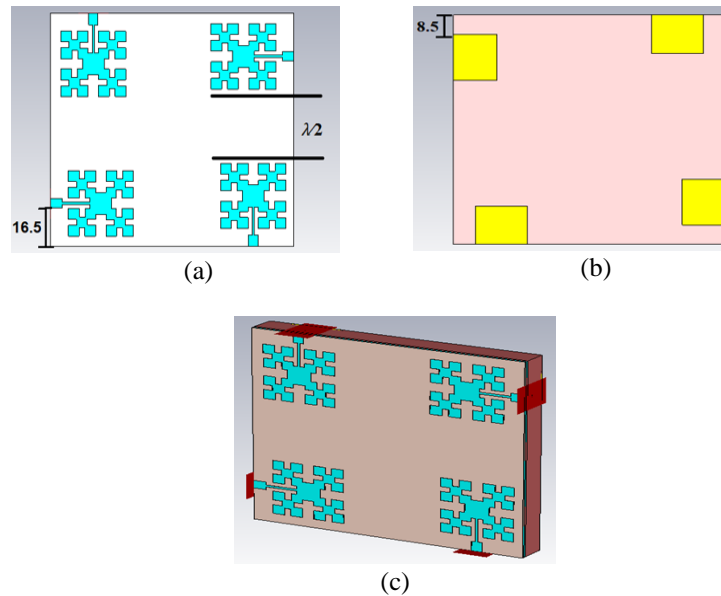


Figure 6. The MIMO antenna design (a) the front view, (b) the back view, and (c) the 3-D view

## 3. RESULTS AND DISCUSSION

### 3.1. S-parameters

At chemical potential  $\mu_c=1$ , the reflection coefficient of the proposed MIMO antenna is less than -10 dB for the band (7.1-13) THz, and the minimum return loss is -30 dB for all S-parameters as illustrated in Figure 7. And the mutual coupling of the four patches in Figure 8 is less than -18 dB for the operating band (7.1-13) THz, with a minimum value close to -70 dB in the active band. At varying the chemical potential values  $\mu_c=0.1, 0.5$ , and  $0.7$ , the reflection coefficient presents a different operational frequency range with other return loss values, so a reconfigurable MIMO antenna appears. These are illustrated in Figures 9-11, respectively.

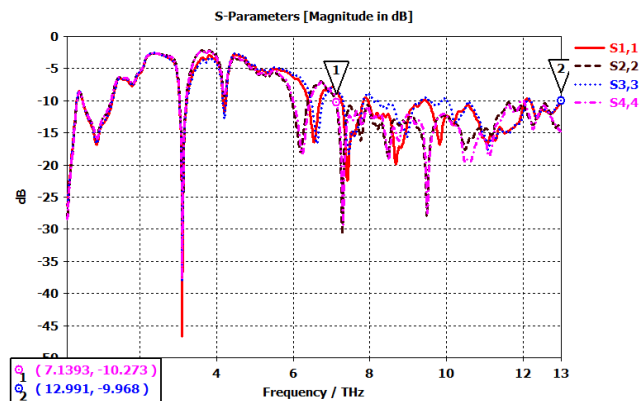


Figure 7. The reflection coefficient of the MIMO antenna

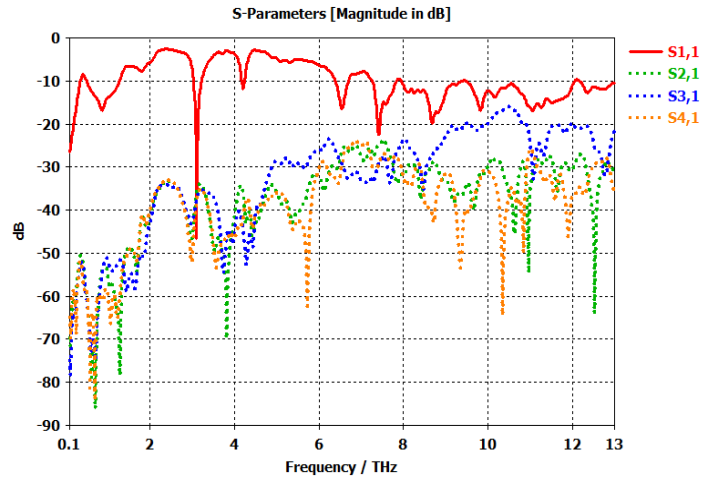


Figure 8. The co-reflection coefficient of the MIMO antenna

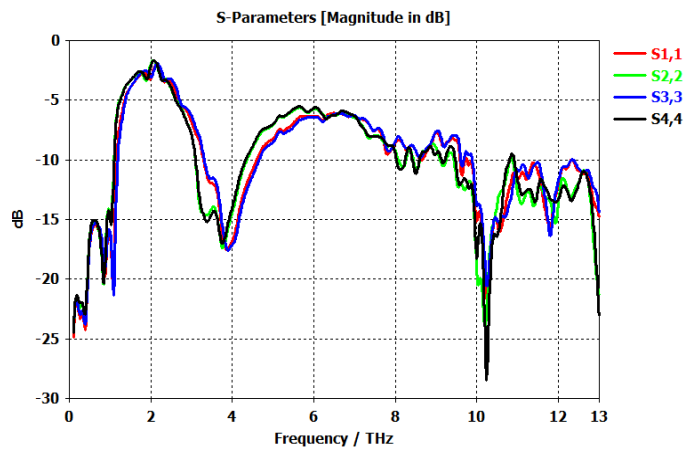


Figure 9. The reflection coefficient at  $\mu c=0.1$

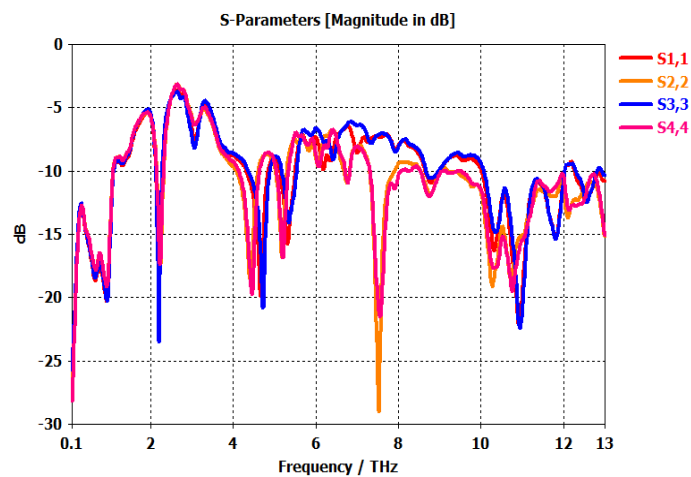


Figure 10. The reflection coefficient at  $\mu c=0.5$

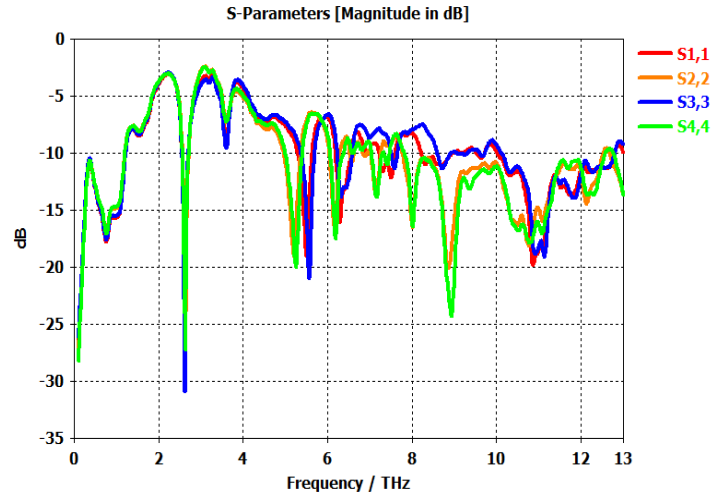


Figure 11. The reflection coefficient at  $\mu_c=0.7$

**3.2. The radiation pattern**

The electric and magnetic field radiation pattern of the designed MIMO antenna is shown in Figures 12-15. The Figures showing the proposed antenna's simulated far-field in the (Y-Z plane) E-plane and (X-Z plane) H-plane at (7-10-12-13) THz. There is little difference in radiation patterns in the different frequencies.

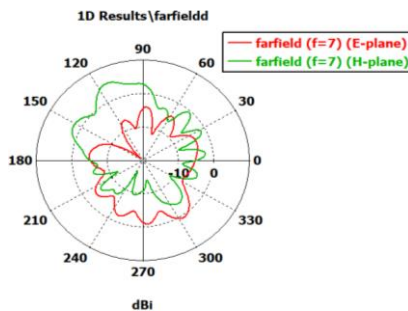


Figure 12. The radiation pattern at 7 THz

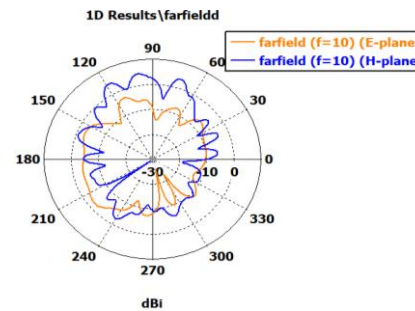


Figure 13. The radiation pattern at 10 THz

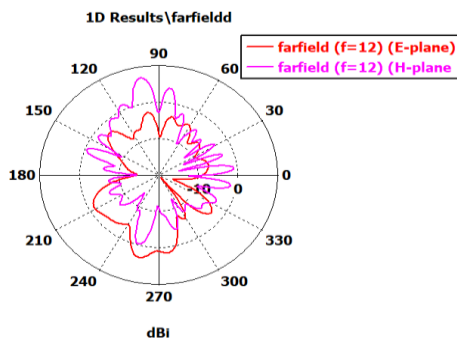


Figure 14. The radiation pattern at 12 THz

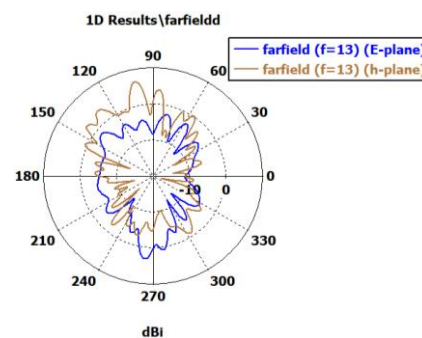


Figure 15. The radiation pattern at 13 THz

**3.3. Gain IEEE, envelop correlation confliction (ECC) and diversity gain (DG)**

Because of the need for a more considerable data rate for long-distance transmission, the MIMO configuration was created to guarantee compatibility of the graphene MIMO antenna in the THz frequency

range. The MIMO antenna's most outstanding gain value is 8.3 dB at 11 THz, As presented in Figure 16. This part will explore essential parameters associated with the designed MIMO antenna, which are pretty important.

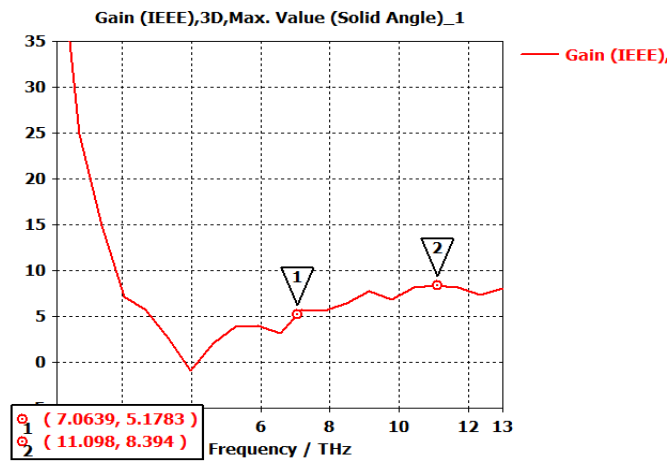


Figure 16. The radiation pattern at 12 THz

The envelope correlation coefficient (ECC) is essential for identifying the correlation between the ports. The ECC value should range from 0 to 0.5 and be very low to show that each channel is independent. MIMO antennas should have a minimum ECC That can be calculated by S-parameter as shown in (5) [25]:

$$|\rho_{(ij)}|^2 = \rho_{(eij)} = \left| \frac{|S_{ii}^* S_{ij} + S_{ji}^* S_{jj}|}{\left[ (1 - |S_{ii}|^2 - |S_{ji}|^2)(1 - |S_{jj}|^2 - |S_{ij}|^2) \eta_{radi} \eta_{radj} \right]^{(1/2)}} \right|^2 \tag{5}$$

where  $S_{ii}^*$  and  $S_{ji}^*$  represent the conjugate of the MIMO antenna's s-parameter. The envelope correlation coefficient ECC is less than 0.005 in the operating band, as illustrated in Figure 17.

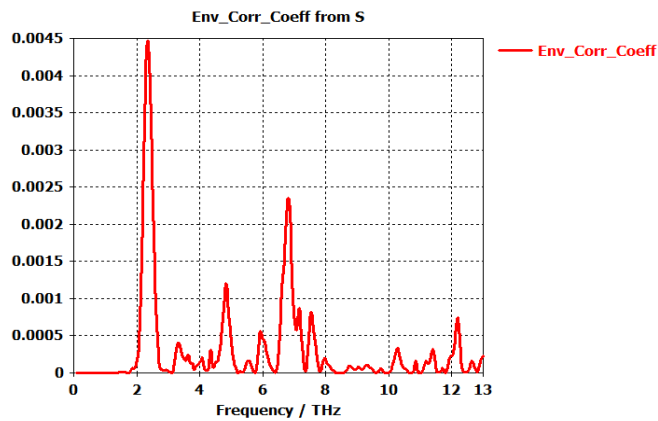


Figure 17. The ECC for the MIMO antenna

The diversity gain, often known as DG, is an additional method that may be used to define the losses caused by the transmitted power. The DG value is computed by making use of the formula that is presented in (6) [25].

$$DG = 10\sqrt{1 - (ECC)^2} \tag{6}$$



The value of the ECC influences the DG, demonstrating that a lower value of the ECC produces an excellent diversity gain value, making the MIMO antenna appropriate for various applications. Figure 18 depicts the diversity gain DG is close to 9.99 dB.

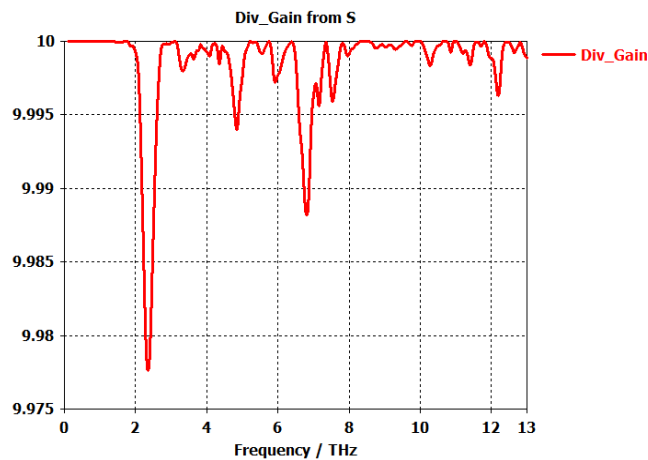


Figure 18. The DG for the MIMO antenna

#### 4. CONCLUSION

This work describes in detail the construction, development, and measurement of a valuable antenna for MIMO applications. A reconfigurable four-element MIMO antenna has been designed and numerically analyzed for THz applications. The graphene MIMO antenna operates at (7.1-13) THz with minimum return loss close to -30 dB. The proposed MIMO antenna displays the highest gain value of 8.3 dB at 11 THz, and ECC is less than 0.005 dB for any two elements. Diversity gain DG value is more significant than 9.97 dB for the band of interest. The MIMO antenna design that has been proposed for usage in the future is capable of functioning as a massive MIMO and makes use of intelligent surfaces that can be reconfigured. That makes it appropriate for use with 6G communication technology. The presented multiple input MIMO antenna is well-suited for high-speed, short-distance indoor communication applications in the terahertz frequency region. These applications include biological imaging, security scanning, sensing, and video-rate imaging.

#### ACKNOWLEDGEMENTS

The authors want to thank Al-Mustansirya University, College of Engineering, Electrical Department, in Baghdad, Iraq, for supporting and helping to produce this work.




#### REFERENCES

- [1] X. Zhou, T. Leng, K. Pan, M. Abdalla, K. S. Novoselov, and Z. Hu, "Conformal screen printed graphene  $4 \times 4$  wideband MIMO antenna on flexible substrate for 5G communication and IoT applications," *2D Materials*, vol. 8, no. 4, p. 045021, Oct. 2021, doi: 10.1088/2053-1583/ac1959.
- [2] A. K. Singh and P. Kaur, "Design of graphene based antenna for 5G MIMO system," in *2019 International Conference on Computing, Power and Communication Technologies, GUCON 2019*, 2019, pp. 503–507.
- [3] M. F. Ali, R. Bhattacharya, and G. Varshney, "Tunable four-port MIMO/self-multiplexing THz graphene patch antenna with high isolation," *Optical and Quantum Electronics*, vol. 54, no. 12, p. 822, Dec. 2022, doi: 10.1007/s11082-022-04200-x.
- [4] S. A. Khaleel, E. K. I. Hamad, N. O. Parchin, and M. B. Saleh, "MTM-inspired graphene-based THz MIMO antenna configurations using characteristic mode analysis for 6G/IoT applications," *Electronics*, vol. 11, no. 14, p. 2152, Jul. 2022, doi: 10.3390/electronics11142152.
- [5] M. Giordani, M. Polese, M. Mezzavilla, S. Rangan, and M. Zorzi, "Toward 6G networks: use cases and technologies," *IEEE Communications Magazine*, vol. 58, no. 3, pp. 55–61, Mar. 2020, doi: 10.1109/MCOM.001.1900411.
- [6] M. Alsabah *et al.*, "6G wireless communications networks: a comprehensive survey," *IEEE Access*, vol. 9, pp. 148191–148243, 2021, doi: 10.1109/ACCESS.2021.3124812.
- [7] M. Z. Chowdhury, M. Shahjalal, S. Ahmed, and Y. M. Jang, "6G wireless communication systems: applications, requirements, technologies, challenges, and research directions," *IEEE Open Journal of the Communications Society*, vol. 1, pp. 957–975, 2020, doi: 10.1109/OJCOMS.2020.3010270.
- [8] R. H. Mahdi, H. A. Abdulnabi, and A. Alsudani, "Plasmonic high gain graphene-based antenna array design for ultra wide band terahertz applications," *Bulletin of Electrical Engineering and Informatics (BEEI)*, vol. 11, no. 6, pp. 3322–3328, Dec. 2022, doi: 10.11591/eei.v11i6.3673.




- [9] G. Geetharamani and T. Aathmanesan, "Split ring resonator inspired THz antenna for breast cancer detection," *Optics and Laser Technology*, vol. 126, p. 106111, Jun. 2020, doi: 10.1016/j.optlastec.2020.106111.
- [10] S. P.-Khanjari and F. B. Zarrabi, "Reconfigurable vivaldi THz antenna based on graphene load as hyperbolic metamaterial for skin cancer spectroscopy," *Optics Communications*, vol. 480, p. 126482, Feb. 2021, doi: 10.1016/j.optcom.2020.126482.
- [11] F. M. Rasheed and H. A. Abdulnabi, "Toothed log periodic graphene-based antenna design for THz applications," *Bulletin of Electrical Engineering and Informatics (BEEI)*, vol. 11, no. 6, pp. 3346–3352, Dec. 2022, doi: 10.11591/eei.v11i6.4256.
- [12] M.-R. Nickpay, M. Danaie, and A. Shahzadi, "Wideband rectangular double-ring nanoribbon graphene-based antenna for terahertz communications," *IETE Journal of Research*, vol. 68, no. 3, pp. 1625–1634, May 2022, doi: 10.1080/03772063.2019.1661801.
- [13] X.-S. Rong, Q.-M. Wan, H.-L. Peng, Y.-P. Zhang, and J.-F. Mao, "A graphene loaded THz patch antenna with tunable frequency," in *2018 IEEE World Symposium on Communication Engineering (WSCE)*, Dec. 2018, pp. 76–79, doi: 10.1109/WSCE.2018.8690534.
- [14] M. A. Ismail, K. M. M. Zaini, and M. I. Syono, "Graphene field-effect transistor simulation with TCAD on top-gate dielectric influences," *Telkonnika (Telecommunication Computing Electronics and Control)*, vol. 17, no. 4, pp. 1845–1852, Aug. 2019, doi: 10.12928/TELKOMNIKA.V17I4.12760.
- [15] H. A. Abdulnabi and Y. Y. Al-Aboosi, "Design of tunable multiband hybrid graphene metal antenna in microwave regime," *Indonesian Journal of Electrical Engineering and Computer Science*, vol. 12, no. 3, pp. 1003–1009, Dec. 2018, doi: 10.11591/ijeecs.v12.i3.pp1003-1009.
- [16] A. G. Alharbi and V. Sorathiya, "Ultra-wideband graphene-based micro-sized circular patch-shaped Yagi-like MIMO antenna for terahertz wireless communication," *Electronics*, vol. 11, no. 9, p. 1305, Apr. 2022, doi: 10.3390/electronics11091305.
- [17] H. A. Abdulnabi, R. T. Hussein, and R. S. Fyath, "UWB Single port log periodic toothed terahertz antenna design based on graphene artificial magnetic conductor," *Modern Applied Science*, vol. 11, no. 3, p. 86, Jan. 2017, doi: 10.5539/mas.v11n3p86.
- [18] G. W. Hanson, A. B. Yakovlev, and A. Mafi, "Excitation of discrete and continuous spectrum for a surface conductivity model of graphene," *Journal of Applied Physics*, vol. 110, no. 11, p. 114305, Dec. 2011, doi: 10.1063/1.3662883.
- [19] F. M. Rasheed and H. A. Abdulnabi, "Multiband graphene-based Mimo antenna in terahertz antenna regime," in *2022 2nd International Conference on Computing and Machine Intelligence, ICMI 2022 - Proceedings*, Apr. 2022, pp. 1–6, doi: 10.1109/ICMI55296.2022.9873789.
- [20] W. M. Abdulkawi, A. F. A. Sheta, I. Elshafiey, and M. A. Alkanhal, "Design of low-profile single-and dual-band antennas for iot applications," *Electronics (Switzerland)*, vol. 10, no. 22, p. 2766, Nov. 2021, doi: 10.3390/electronics10222766.
- [21] A. F. Sheta, N. Dib, and A. Mohra, "Investigation of new nondegenerate dual-mode microstrip patch filter," *IEE Proceedings: Microwaves, Antennas and Propagation*, vol. 153, no. 1, pp. 89–95, 2006, doi: 10.1049/ip-map:20050103.
- [22] H. A. Abdulnabi, Y. Y. Al-Aboosi, and A. H. Sallomi, "Photonic antenna design for long term evolution application," *IOP Conference Series: Materials Science and Engineering*, vol. 881, no. 1, p. 012147, Jul. 2020, doi: 10.1088/1757-899X/881/1/012147.
- [23] Z. Du, K. Gong, J. S. Fu, and B. Gao, "Analysis of microstrip fractal patch antenna for multi-band communication," *Electronics Letters*, vol. 37, no. 13, pp. 805–806, 2001, doi: 10.1049/el:20010570.
- [24] N. Hussain, W. A. Awan, W. Ali, S. I. Naqvi, A. Zaidi, and T. T. Le, "Compact wideband patch antenna and its MIMO configuration for 28 GHz applications," *AEU - International Journal of Electronics and Communications*, vol. 132, p. 153612, Apr. 2021, doi: 10.1016/j.aeue.2021.153612.
- [25] K. V. Babu, S. Das, G. Varshney, G. N. J. Sree, and B. T. P. Madhav, "A micro-scaled graphene-based tree-shaped wideband printed MIMO antenna for terahertz applications," *Journal of Computational Electronics*, vol. 21, no. 1, pp. 289–303, Feb. 2022, doi: 10.1007/s10825-021-01831-3.

## BIOGRAPHIES OF AUTHORS



**Reem Hikmat Abd**    received a B.Eng. degree in information engineering from Al-Nahrain University Baghdad/Iraq, in 2011. She is currently Emp. in information technology department, ministry of transportation. She can be contacted at email: reem.engineer89@gmail.com.



**Hussein A. Abdulnabi**    received the B.Eng. degree in electrical engineering from Al-Rasheed College Baghdad, Iraq, in 1991, and the master's degree in electronic and communication engineering science from Al-Mustansiriyah University in 2000 and the Ph.D. degree in communication engineering from the University of Technology, Iraq in 2017. He is currently a Assoc. Prof. in Electrical Engineering Department, Al-Mustansiriyah University. His current research interests include communication, antenna design. He can be contacted at email: ali682@yahoo.com.